

[文章编号] 1671-587X(2026)01-0081-12

DOI:10.13481/j.1671-587X.20260109

抑制 *miR-17-5p* 通过靶向调控 *Mfn2* 表达对划痕损伤引起大鼠 脊髓星形胶质细胞增殖的抑制作用

赵 焱, 吴华伟

(湖北省武汉市第四医院神经外科, 湖北 武汉 430030)

[摘要] **目的:** 探讨抑制微小RNA(*miR*)-17-5*p*对划痕损伤诱导大鼠星形胶质细胞增殖的影响,并阐明其作用机制。**方法:** 原代分离培养大鼠脊髓组织中的星形胶质细胞,将*miR-17-5p*抑制剂(*miR-17-5p* inhibitor)及其阴性对照(inhibitor-NC)和线粒体融合蛋白2(*Mfn2*)干扰质粒(*si-Mfn2*)及其阴性对照(*si-NC*)转染至大鼠脊髓星形胶质细胞中,采用划痕法建立体外机械损伤诱导的星形胶质细胞增殖模型。将星形胶质细胞分为对照组(不进行处理)、Scratch组(划痕处理)、Scratch+inhibitor-NC组(转染inhibitor-NC后划痕处理)和Scratch+*miR-17-5p* inhibitor组(转染*miR-17-5p* inhibitor后划痕处理)以及空白组(不进行处理)、inhibitor-NC组(转染inhibitor-NC)、*miR-17-5p* inhibitor组(转染*miR-17-5p* inhibitor)、*miR-17-5p* inhibitor+*si-NC*组(共转染*miR-17-5p* inhibitor和*si-NC*后划痕处理)和*miR-17-5p* inhibitor+*si-Mfn2*组(共转染*miR-17-5p* inhibitor和*si-Mfn2*后划痕处理)。采用细胞划痕愈合实验检测不同时间点划痕愈合率,实时荧光定量PCR(RT-qPCR)法检测各组细胞中*miR-17-5p*和*Mfn2* mRNA表达水平,Western blotting法检测各组细胞中*Mfn2*、胶质纤维酸性蛋白(GFAP)、增殖细胞核抗原(PCNA)和Ki-67蛋白表达水平,免疫荧光法检测各组细胞中GFAP和Ki-67表达情况,5-溴-2'-脱氧尿苷(BrdU)实验检测各组细胞增殖情况,双荧光素酶报告基因实验验证*Mfn2*和*miR-17-5p*之间的靶向关系。**结果:** 细胞划痕愈合实验,随着划痕损伤时间(0、12、24和48 h)的延长,大鼠脊髓星形胶质细胞划痕愈合率升高($P<0.05$),且呈时间依赖性。RT-qPCR法和Western blotting法,与Scratch 0 h组比较,Scratch 12、24和48 h组大鼠星形胶质细胞中*miR-17-5p*表达水平以及GFAP、PCNA和Ki-67蛋白表达水平升高($P<0.05$),*Mfn2*蛋白表达水平降低($P<0.05$),且呈时间依赖性;与对照组比较,Scratch组星形胶质细胞中GFAP和Ki-67蛋白表达水平升高($P<0.05$),*Mfn2*蛋白表达水平降低($P<0.05$);与Scratch组比较,Scratch+*miR-17-5p* inhibitor组星形胶质细胞中GFAP和Ki-67蛋白表达水平降低($P<0.05$),*Mfn2*蛋白表达水平升高($P<0.05$);与空白组比较,*miR-17-5p* inhibitor组星形胶质细胞中*miR-17-5p*表达水平降低($P<0.05$),*Mfn2* mRNA和蛋白表达水平升高($P<0.05$);与Scratch+*miR-17-5p* inhibitor组比较,*miR-17-5p* inhibitor+*si-Mfn2*组星形胶质细胞中*Mfn2*蛋白表达水平降低($P<0.05$)。免疫荧光法,与对照组比较,Scratch组GFAP和Ki-67共定位星形胶质细胞数量增加($P<0.05$);与Scratch组比较,Scratch+*miR-17-5p* inhibitor组GFAP和Ki-67共定位星形胶质细胞数量减少($P<0.05$);与Scratch+*miR-17-5p* inhibitor组比较,*miR-17-5p* inhibitor+*si-Mfn2*组GFAP和Ki-67共定位星形胶质细胞数量增加($P<0.05$)。BrdU实验,与对照组比较,Scratch组星形胶质细胞BrdU阳性表达率升高($P<0.05$);与Scratch组比较,Scratch+*miR-17-5p* inhibitor组星形胶质细胞BrdU阳性表达率降低($P<0.05$);与Scratch+*miR-17-5p* inhibitor组比较,*miR-17-5p* inhibitor+*si-Mfn2*组星形胶质细胞BrdU阳

[收稿日期] 2025-04-08 [录用日期] 2025-05-24

[基金项目] 湖北省科技厅自然科学基金项目(2023AFB994)

[作者简介] 赵 焱(1976—),男,湖北省武汉市人,副主任医师,医学硕士,主要从事脊柱脊髓损伤及修复方面的研究。

[通信作者] 吴华伟,副主任医师(E-mail: coordinate999@163.com)

©《吉林大学学报(医学版)》编辑部,开放获取遵循CC BY-NC-ND协议。

© Editorial Board of Journal of Jilin University (Medicine Edition). Open access under CC BY-NC-ND license.

性表达率升高 ($P < 0.05$)。双荧光素酶报告基因实验, *miR-17-5p* 和 *Mfn2* mRNA 的 3'UTR 区存在结合位点, *Mfn2* 是 *miR-17-5p* 下游靶基因。**结论:** 大鼠脊髓星形胶质细胞划痕损伤后细胞中 *miR-17-5p* 表达水平明显升高, 细胞增殖活性增加, 抑制 *miR-17-5p* 通过靶向上调 *Mfn2* 表达抑制划痕损伤所致星形胶质细胞的增殖。

[关键词] 星形胶质细胞; 划痕损伤; 细胞增殖; 微小RNA-17-5p; 线粒体融合蛋白2

[中图分类号] R681.5 [文献标志码] A

Inhibitory effect of inhibition of miR-17-5p on proliferation of spinal cord astrocytes of rats induced by scratch injury through targeting Mfn2 expression

ZHAO Yan, WU Huawei

(Department of Neurosurgery, Fourth Hospital, Wuhan City, Hubei Province, Wuhan 430033, China)

ABSTRACT Objective: To discuss the effect of inhibiting micro RNA (*miR*)-17-5p on scratch injury-induced proliferation of rat astrocytes and to clarify its mechanism. **Methods:** The astrocytes were isolated and cultured primarily from rat spinal cord tissue. *MiR-17-5p* inhibitor and its negative control (inhibitor-NC), and mitofusin 2 (*Mfn2*) interfering plasmid (si-*Mfn2*) and its negative control (si-NC) were transfected into rat spinal cord astrocytes. An in vitro mechanical injury-induced astrocyte proliferation model was established using the scratch method. Astrocytes were divided into control group (no treatment), Scratch group (scratch treatment), Scratch+inhibitor-NC group (transfected with inhibitor-NC then scratch treatment), and Scratch+*miR-17-5p* inhibitor group (transfected with *miR-17-5p* inhibitor then scratch treatment); and also into blank group (no treatment), inhibitor-NC group (transfected with inhibitor-NC), *miR-17-5p* inhibitor group (transfected with *miR-17-5p* inhibitor), *miR-17-5p* inhibitor+si-NC group (co-transfected with *miR-17-5p* inhibitor and si-NC then scratch treatment), and *miR-17-5p* inhibitor+si-*Mfn2* group (co-transfected with *miR-17-5p* inhibitor and si-*Mfn2* then scratch treatment). Cell scratch healing assay was used to detect the scratch healing rates at different time points; real-time fluorescence quantitative PCR (RT-qPCR) method was used to detect the *miR-17-5p* and *Mfn2* mRNA expression levels in the cells in various groups; Western blotting method was used to detect the protein expression levels of *Mfn2*, glial fibrillary acidic protein (GFAP), proliferating cell nuclear antigen (PCNA), and proliferation marker protein Ki-67 in the cells in various groups; immunofluorescence method was used to detect the expression of GFAP and Ki-67 in the cells in various groups; 5-bromo-2'-deoxyuridine (BrdU) assay was used to detect the proliferation of cells in various groups; the dual-luciferase reporter gene assay were used to verify the targeted regulatory relationship between *Mfn2* and *miR-17-5p*. **Results:** The cell scratch healing assay results showed that as the scratch injury time (0, 12, 24, and 48 h) increased, the scratch healing rate of spinal cord astrocytes of the rats was increased ($P < 0.05$) in a time-dependent manner. The RT-qPCR and Western blotting results showed that compared with Scratch 0 h group, the *miR-17-5p* expression level and the protein expression levels of GFAP, PCNA, and Ki-67 in astrocytes in Scratch 12, 24, and 48 h groups were increased ($P < 0.05$), while the *Mfn2* protein expression level was decreased ($P < 0.05$) in a time-dependent manner; compared with Control group, the GFAP and Ki-67 protein expression levels in astrocytes in Scratch group were increased ($P < 0.05$), while the *Mfn2* protein expression level was decreased ($P < 0.05$); compared with Scratch group, the GFAP and Ki-67 protein expression levels in astrocytes in Scratch+*miR-17-5p* inhibitor group were decreased ($P < 0.05$), while the *Mfn2* protein expression level was increased ($P < 0.05$); compared with blank group, the *miR-17-5p*

expression level in astrocytes in *miR-17-5p* inhibitor group was decreased ($P < 0.05$), while the Mfn2 mRNA and protein expression levels were increased ($P < 0.05$); compared with Scratch+*miR-17-5p* inhibitor group, the Mfn2 protein expression level in astrocytes in *miR-17-5p* inhibitor+si-Mfn2 group was decreased ($P < 0.05$). The immunofluorescence assay results showed that compared with control group, the numbers of GFAP and Ki-67 co-localized astrocytes in Scratch group was increased ($P < 0.05$); compared with Scratch group, the number of GFAP and Ki-67 co-localized astrocytes in scratch+*miR-17-5p* inhibitor group was decreased ($P < 0.05$); compared with Scratch+*miR-17-5p* inhibitor group, the number of GFAP and Ki-67 co-localized astrocytes in *miR-17-5p* inhibitor+si-Mfn2 group was increased ($P < 0.05$). The BrdU assay results showed that compared with control group, the BrdU positive expression rate in the astrocytes in Scratch group was increased ($P < 0.05$); compared with scratch group, the BrdU positive expression rate in astrocytes in Scratch+*miR-17-5p* inhibitor group was decreased ($P < 0.05$); compared with scratch+*miR-17-5p* inhibitor group, the BrdU positive expression rate in astrocytes in *miR-17-5p* inhibitor+si-Mfn2 group was increased ($P < 0.05$). The dual-luciferase reporter gene assay results showed that there was a binding site between *miR-17-5p* and the 3'UTR region of *Mfn2* mRNA, and *Mfn2* is a downstream target gene of *miR-17-5p*. **Conclusion:** The *miR-17-5p* expression level in rat spinal cord astrocytes is significantly increased after scratch injury, and cell proliferation activity is increased. Inhibition of *miR-17-5p* suppresses the proliferation of astrocytes induced by scratch injury by targeting and upregulating Mfn2 expression.

KEYWORDS Astrocyte; Scratch injury; Cell proliferation; MicroRNA-17-5p; Mitofusin 2

脊髓损伤通常是由高处坠落伤、交通事故和腰背部外力撞击等因素致使脊柱骨折、脱位造成, 脊髓的轴突网络被破坏、出血和炎症等多种损伤表现持续恶化最终可导致瘫痪^[1]。胶质瘢痕形成是影响轴突再生的重要外部因素, 其主要成分为病变周围的肥大反应性星形胶质细胞, 脊髓损伤后星形胶质细胞增殖形成的胶质瘢痕构成物理屏障并抑制轴突生长^[2]。线粒体融合蛋白 2 (mitofusin 2, Mfn2) 是一种定位于线粒体外膜和内质网表面的跨膜蛋白, 通过影响线粒体的融合和分裂, 参与细胞增殖、凋亡及氧化应激等多种生理病理过程^[3]。CAO 等^[4]研究显示: 在脊髓损伤后 3 和 6 h, 大鼠脊髓损伤处神经元中线粒体数量显著减少, 并伴随线粒体融合相关基因 *Mfn2* 的表达下调, 但 12 和 24 h 后则呈现相反趋势。SHI 等^[5] 研究显示: 过表达 Mfn2 可有效抑制星形胶质细胞的增殖并阻滞细胞周期, 提示 Mfn2 可能是治疗脊髓损伤的潜在靶点。微小 RNA (microRNA, miRNA) 是一类内生的小 RNA, 通过调控 1 个或多个靶基因参与细胞周期的调节。HONG 等^[6] 研究显示: *miR-17-5p* 家族成员 (包括 *miR-17-5p*) 在脊髓损伤期间显著上调, 且抑制 *miR-17-5p* 表达可阻断机械损伤诱导的星形胶质细胞增殖。ZHANG 等^[7] 研究显示: *miR-17-5p* 可以靶向原代感觉神经元中的信号转导和转录激活因

子 3 (signal transducer and activator of transcription 3, STAT3), 在调节皮层神经元轴突生长中发挥关键作用。上述研究表明: *miR-17-5p* 可能参与星形胶质细胞病理性增殖过程, 是改善胶质瘢痕的潜在靶点, 但其是否通过调控 Mfn2 在脊髓损伤后的胶质瘢痕形成中发挥作用, 目前尚不明确。本研究采用划痕法建立体外机械损伤诱导的大鼠脊髓星形胶质细胞增殖模型, 探讨下调 *miR-17-5p* 对划痕损伤诱导大鼠星形胶质细胞增殖的影响及机制, 以期以 *miR-17-5p* 作为脊髓损伤的治疗靶点提供依据。

1 材料与方法

1.1 实验动物、主要试剂和仪器

20 只 SPF 级 SD 大鼠, 雌雄各半, 8 周龄, 购自斯贝福 (北京) 生物技术有限公司, 动物生产许可证号: SCXK (京) 2024-0001。将大鼠进行合笼交配, 取新生 0~2 d 大鼠幼崽用于原代分离。本研究获得武汉贝赛模式生物中心实验动物福利伦理委员会的批准 [批准号: BSMS 动 (福) 第 2024-11-22A 号]。Dulbecco's 改良培养基 (Dulbecco's modified eagle medium, DMEM) 和胎牛血清购自武汉普诺赛生命科技有限公司, 1% 青-链霉素混合液购自北京索莱宝科技有限公司, *miR-17-5p* 抑制剂 (*miR-17-5p* inhibitor) 及其阴性对照 (inhibitor-NC)、Mfn2 干扰质粒 (si-Mfn2) 及其阴性对照 (si-NC) 和双荧

光素酶检测试剂盒购自武汉金开瑞生物工程有限公司,兔抗胶质纤维酸性蛋白(glia fibrillary acidic protein, GFAP)、兔抗Ki-67、兔抗Mfn2、鼠抗增殖细胞核抗原(proliferating cell nuclear antigen, PCNA)和鼠抗5-溴-2'-脱氧尿苷(5-bromo-2'-deoxyuridine, BrdU)抗体购自英国Abcam公司,Hiief Trans[®]小干扰RNA(small interfering RNA, siRNA)/miRNA体外转染试剂购自上海翌圣生物科技股份有限公司, BrdU($\geq 99\%$)和BeyoFast[™] SYBR Green One-Step实时荧光定量PCR(real time fluorescence quantitative PCR, RT-qPCR)试剂盒购自上海碧云天生物技术研究所。荧光显微镜(型号: BX53)购自日本OLYMPUS公司, RT-qPCR系统和凝胶成像系统(型号: ProFlex[™]、iBright[™] CL1500)购自美国ThermoFisher公司。

1.2 原代星形胶质细胞分离和培养 参考文献[8]方法,采用异氟烷吸入麻醉法麻醉大鼠幼崽,迅速断头,于背部切口暴露脊柱,使用显微剪和显微镊切开脊柱,轻柔剥离脊髓放入预冷的无血清DMEM培养基中。制备单细胞悬液,在37℃的细胞培养箱中进行培养,每3 d换液1次,第12天时可见小胶质细胞群在星形胶质细胞顶部生长。将细胞置于轨道振荡器上以250 r·min⁻¹转速持续震荡3 h,吸出包含从星形胶质细胞顶部脱落的黏附性较差的小胶质细胞的培养基,磷酸盐缓冲溶液(phosphate buffered saline, PBS)洗涤底部星形胶质细胞层,继而加入0.25%胰酶孵育1 min,然后将细胞重悬于含有10%胎牛血清和1%青-链霉素的DMEM培养基中继续培养,后续采用免疫荧光法对分离培养的细胞进行鉴定。

1.3 采用RT-qPCR法和Western blotting法检测各组细胞转染效率 按照试剂盒说明书要求,配制含有miR-17-5p inhibitor、inhibitor-NC、si-Mfn2和si-NC的阳离子核酸转染试剂复合物。转染前1 d接种星形胶质细胞于6孔细胞培养板中,待细胞密度达70%时,加入2 mL预配制的复合物,置于CO₂培养箱中培养48 h,采用RT-qPCR法和Western blotting法检测各组细胞转染效率。

1.4 划痕法制备细胞划痕损伤模型、细胞分组和处理 取处于对数生长期的星形胶质细胞,采用划痕法建立体外机械损伤诱导的星形胶质细胞增殖模型^[9],并进行以下分组及处理。在第1部分实验中,分别对星形胶质细胞进行划痕损伤0、12、24和

48 h处理,作为Scratch 0 h组、Scratch 12 h组、Scratch 24 h组和Scratch 48 h组;在第2部分实验中,分别将inhibitor-NC和miR-17-5p inhibitor转染至星形胶质细胞中,随后进行划痕损伤48 h处理,作为Scratch+inhibitor-NC组和Scratch+miR-17-5p inhibitor组,未经转染的细胞作为对照组和Scratch组;在第3部分实验中,分别将inhibitor-NC和miR-17-5p inhibitor转染至星形胶质细胞中,随后正常培养48 h,作为inhibitor-NC组和miR-17-5p inhibitor组,未经转染的细胞设置为空白组;在第4部分实验中,miR-17-5p inhibitor分别与si-NC或si-Mfn2共转染至星形胶质细胞中,随后进行划痕损伤48 h处理,作为miR-17-5p inhibitor+si-NC组和miR-17-5p inhibitor+si-Mfn2组。

1.5 细胞划痕愈合实验检测不同时间点划痕愈合率 收集处于对数生长期的细胞接种于6孔细胞培养板中,按分组要求处理后分别于划痕0、12、24和48 h后观察伤口愈合情况,显微镜下观察并拍照,采用Image J软件分析划痕面积,计算划痕愈合率。划痕愈合率=(0 h划痕面积-终点时间划痕面积)/0 h划痕面积 $\times 100\%$ 。

1.6 RT-qPCR法检测各组细胞中miR-17-5p和Mfn2 mRNA表达水平 收集处于对数生长期的细胞接种于6孔细胞培养板中,按分组要求处理后使用TRIzol试剂从细胞沉淀中提取总RNA。取2 μ g总RNA按照试剂盒说明书操作合成cDNA,将cDNA与目的基因引物(miR-17-5p引物序列:上游引物,5'-GTGCTTACAGTGCAGGTAGGT-3',下游引物,5'-TGTCGTGGAGTCGGCAATTG-3'; Mfn2引物序列:上游引物,5'-AGAGGCGATTTGAGGAGTGC-3',下游引物,5'-CCTCCTCCGTGACCCTCCTTGATC-3'; U6引物序列:上游引物,5'-CTCGCTTCGGCAGCACATATACTA-3',下游引物,5'-ACGAATTTGCGTGTTCATCCTTGCG-3'; GAPDH引物序列:上游引物,5'-CAAGCTCATTTCCCTGGTATGAC-3',下游引物,5'-CAGTGAGGGTCTCTCTCTTCCCT-3')混合进行PCR扩增反应,反应条件:95℃预变性1 min,95℃变性30 s,60℃退火30 s,72℃延伸1 min,共40个循环。以GAPDH或U6为内参,采用2^{- $\Delta\Delta$ Ct}法计算目的基因表达水平。

1.7 Western blotting法检测各组细胞中Mfn2、GFAP、Ki-67和PCNA蛋白表达水平 收集处于对

数生长期的细胞接种于6孔细胞培养板中,按分组要求处理后加入RIPA裂解液于冰上裂解细胞3 min,期间反复吹打以保证细胞完全裂解,12 000 r·min⁻¹离心10 min得到上清即为总蛋白溶液。取20 μg的95 °C变性后蛋白上样于电泳槽,恒压200 V进行十二烷基硫酸钠-聚丙烯酰胺凝胶电泳(sodium dodecyl sulfate-polyacrylamide gel electrophoresis, SDS-PAGE)30 min,恒流300 mA条件下将蛋白转至聚偏氟乙烯(polyvinylidene fluoride, PVDF)膜上,Tris缓冲盐溶液吐温(Tris-buffered saline tween, TBST)洗膜1次,加入5%脱脂牛奶封闭1 h,加入1:1 000稀释后一抗(兔抗Mfn2、GFAP、Ki-67和GAPDH,鼠抗PCNA)摇床过夜, TBST溶液洗膜3次,加入1:5 000稀释后二抗(辣根过氧化物酶标记)室温孵育30 min,增强型化学发光(enhanced chemiluminescence, ECL)液显色,凝胶成像系统扫描胶片,采用Image J分析蛋白条带灰度值,以GAPDH为内参,计算目的蛋白表达水平。目的蛋白表达水平=目的蛋白条带灰度值/内参蛋白条带灰度值。

1.8 免疫荧光法检测各组细胞中GFAP和Ki-67蛋白表达 收集处于对数生长期的细胞接种于6孔细胞培养板中,按分组要求处理后弃上清,加入4%多聚甲醛固定细胞,加入破膜液室温孵育20 min,加入5%牛血清白蛋白室温封闭1 h,加入1:200稀释的一抗(鼠抗GFAP,兔抗Ki-67)混合试剂于4 °C冰箱孵育过夜,加入与一抗相应种属的1:200稀释二抗室温孵育1 h, PBS缓冲液洗涤3次,加入含4',6-二脒基-2-苯基吲哚(4',6-diamidino-2-phenylindole, DAPI)的抗荧光衰减封片剂室温孵育10 min,于不同通道下采集图像,观察划痕处细胞中GFAP和Ki-67共定位情况。

1.9 BrdU实验检测各组细胞增殖能力 收集处于对数生长期的细胞接种于6孔细胞培养板中,按分组要求处理后弃上清,加入4%多聚甲醛固定细胞,随后依次加入盐酸工作液孵育40 min、3%牛血清白蛋白封闭30 min、1:250稀释的BrdU抗体孵育过夜, PBS缓冲液洗涤3次,加入与一抗相应种属的1:1 000稀释二抗孵育50 min,加入DAPI的抗荧光衰减封片剂室温孵育10 min,于不同通道下采集图像,计算细胞中BrdU阳性表达率。阳性表达率=BrdU红色阳性细胞数/DAPI蓝色阳性细

胞数×100%。

1.10 双荧光素酶报告基因实验验证 *miR-17-5p* 与 *Mfn2* 的靶向关系 使用生物信息学网站TargetScan 7.2(http://www.targetscan.org/vert_72/)预测 *miR-17-5p* 和 *Mfn2* 基因之间的靶向结合位点。分别构建 *Mfn2* 的3'UTR区突变型(mutant type, MUT)和野生型(wild type, WT)荧光素酶报告基因载体,将Mfn2-WT和Mfn2-MUT分别与mimics NC和miR-17-5p mimics共转染至大鼠脊髓星形胶质细胞中,荧光素酶活性试剂盒检测各组细胞荧光素酶活性。荧光素酶活性=萤火虫荧光素酶活性/海肾荧光素酶活性。

1.11 统计学分析 采用SPSS 26.0软件进行统计学分析。各组细胞划痕愈合率、BrdU阳性表达率以及 *miR-17-5p*、*Mfn2*、*GFAP*、*PCNA* 和 *Ki-67* mRNA及蛋白表达水平均符合正态分布,以 $\bar{x} \pm s$ 表示,多组间样本均数比较采用单因素方差分析,组间样本均数两两比较采用LSD-*t*检验。所有实验均进行3次生物学重复。以 $P < 0.05$ 为差异有统计学意义。

2 结果

2.1 大鼠脊髓星形胶质细胞的鉴定 原代分离并培养得到纯化的大鼠脊髓星形胶质细胞,细胞边界清晰,从胞体发出许多长而分支的突起,细胞核呈卵圆形,且细胞中GFAP呈阳性表达。见图1。

2.2 划痕损伤不同时间点大鼠脊髓星形胶质细胞划痕愈合率 Scratch 0、12、24和48 h组大鼠脊髓星形胶质细胞划痕愈合率分别为0.00%±0.00%、28.64%±1.92%、56.86%±1.42%和78.69%±3.06%。与Scratch 0 h组比较,Scratch 12、24和48 h组大鼠脊髓星形胶质细胞划痕愈合率明显升高($P < 0.05$),呈时间依赖性。见图2。

2.3 划痕损伤不同时间点大鼠脊髓星形胶质细胞中 *miR-17-5p* 表达水平以及GFAP、PCNA和Ki-67蛋白表达水平 Scratch 0、12、24和48 h组大鼠脊髓星形胶质细胞中 *miR-17-5p* 表达水平分别为1.00±0.03、1.67±0.12、2.47±0.18和3.16±0.26。与Scratch 0 h组比较,Scratch 12、24和48 h组大鼠脊髓星形胶质细胞中 *miR-17-5p* 表达水平以及GFAP、PCNA和Ki-67蛋白表达水平升高($P < 0.05$);与Scratch 12 h组比较,Scratch 24和48 h组大鼠脊髓星形胶质细胞中 *miR-17-5p* 表达水平以及GFAP、PCNA和Ki-67蛋白表达水平升高($P < 0.05$);与Scratch 24 h组比较,Scratch 48 h组大鼠脊髓星形

胶质细胞中 *miR-17-5p* 表达水平以及 GFAP、PCNA 和 Ki-67 蛋白表达水平升高 ($P < 0.05$)。见图 3。

2.4 抑制 *miR-17-5p* 后划痕损伤大鼠脊髓星形胶质细胞中 GFAP 和 Ki-67 免疫荧光共定位情况 图 4 中箭头所指为 GFAP 和 Ki-67 共定位细胞, 对照组、Scratch 组、Scratch+inhibitor-NC 和 Scratch+*miR-17-5p* inhibitor 组大鼠脊髓星形胶质细胞中 GFAP 和 Ki-67 共定位细胞数量分别为 26.00 ± 2.65 、 135.33 ± 9.02 、 128.67 ± 7.51 和 54.00 ± 3.61 。与对照组比较, Scratch 组大鼠脊髓星形胶质细胞中 GFAP 和

Ki-67 共定位细胞数量增加 ($P < 0.05$); 与 Scratch 组比较, Scratch+*miR-17-5p* inhibitor 组大鼠脊髓星形胶质细胞中 GFAP 和 Ki-67 共定位细胞数量减少 ($P < 0.05$), Scratch+inhibitor-NC 组大鼠脊髓星形胶质细胞中 GFAP 和 Ki-67 共定位细胞数量无明显变化, 差异无统计学意义 ($P > 0.05$)。见图 4。

2.5 抑制 *miR-17-5p* 后划痕损伤大鼠脊髓星形胶质细胞中 BrdU 阳性表达率以及 Mfn2、GFAP 和 Ki-67 蛋白表达水平 对照组、Scratch 组、Scratch+inhibitor-NC 组和 Scratch+*miR-17-5p* inhibitor 组大

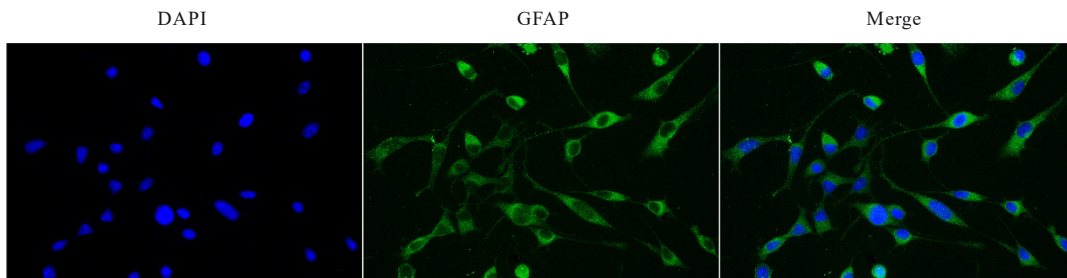


图 1 大鼠脊髓星形胶质细胞中 GFAP 表达情况(免疫荧光法, $\times 400$)

Fig. 1 Expression of GFAP in spinal cord astrocytes of rats (Immunofluorescence, $\times 400$)

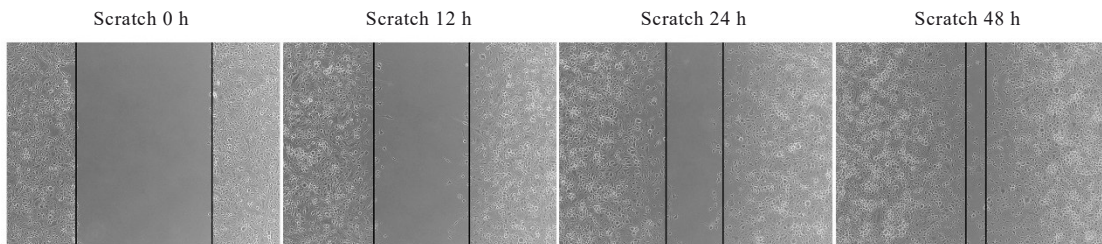
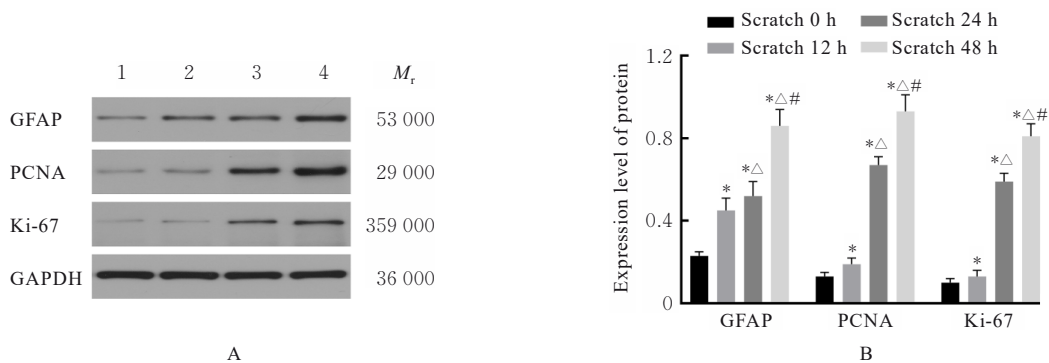


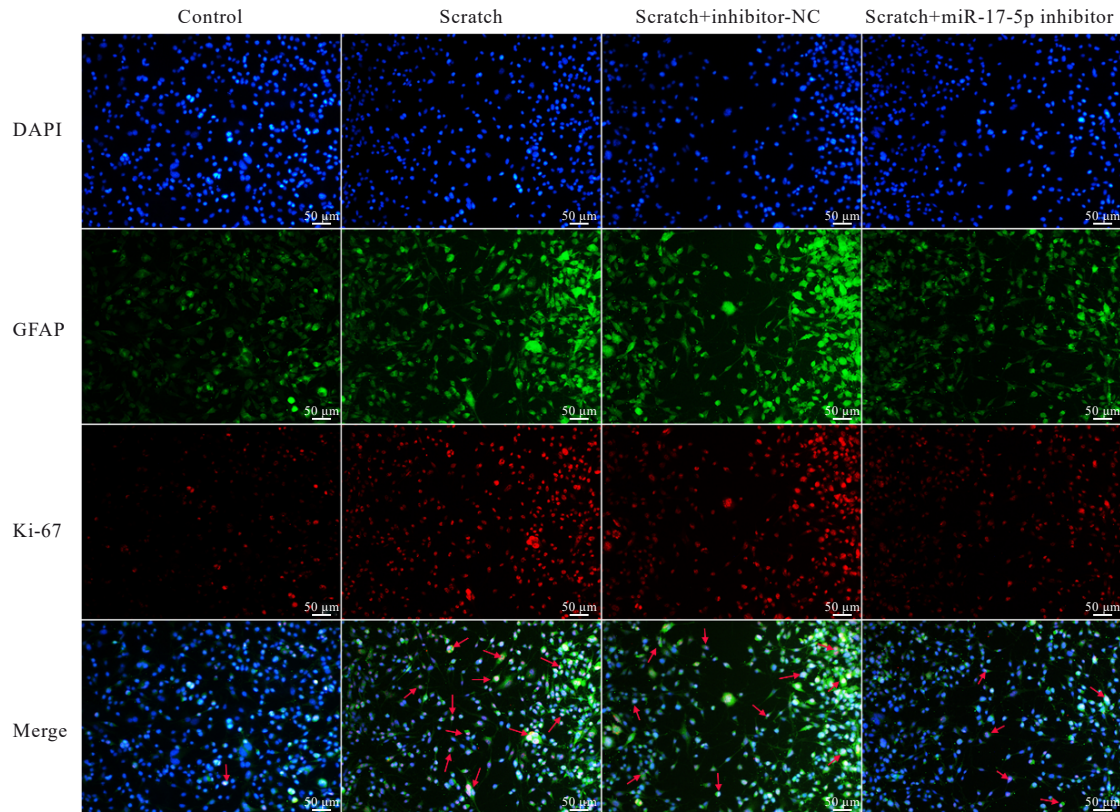
图 2 划痕损伤不同时间点的大鼠脊髓星形胶质细胞愈合情况($\times 40$)

Fig. 2 Cell healing of spinal cord astrocytes of rats at different time points($\times 40$)



Lane 1: Scratch 0 h group; Lane 2: Scratch 12 h group; Lane 3: Scratch 24 h group; Lane 4: Scratch 48 h group. * $P < 0.05$ compared with scratch 0 h group; $\Delta P < 0.05$ compared with scratch 12 h group; # $P < 0.05$ compared with scratch 24 h group.

图 3 划痕损伤不同时间点大鼠脊髓星形胶质细胞中 GFAP、PCNA 和 Ki-67 蛋白表达电泳图(A)及直条图(B)
Fig. 3 Electrophoregram(A) and histogram (B) of expressions of GFAP, PCNA, and Ki-67 proteins in spinal cord astrocytes of rats at different time points



Arrows referred to GFAP and Ki-67 co-localized cells.

图4 各组大鼠脊髓星形胶质细胞中GFAP和Ki-67免疫荧光共定位情况

Fig. 4 Immunofluorescence co-localization of GFAP and Ki-67 in spinal cord astrocytes of rats in various groups

鼠脊髓星形胶质细胞中BrdU阳性表达率分别为 $4.58\% \pm 0.62\%$ 、 $76.20\% \pm 6.55\%$ 、 $72.18\% \pm 7.14\%$ 和 $25.36\% \pm 3.05\%$ 。与对照组比较, Scratch组大鼠脊髓星形胶质细胞中BrdU阳性表达率以及GFAP和Ki-67蛋白表达水平升高 ($P < 0.05$), *Mfn2* 蛋白表达水平降低 ($P < 0.05$)。与Scratch组比较, Scratch+*miR-17-5p* inhibitor组大鼠脊髓星形胶质细胞中BrdU阳性表达率以及GFAP和Ki-67蛋白表达水平降低 ($P < 0.05$), *Mfn2* 蛋白表达水平升高 ($P < 0.05$); Scratch组与Scratch+inhibitor-NC组大鼠脊髓星形胶质细胞中BrdU阳性表达率以及GFAP、Ki-67和*Mfn2*蛋白表达水平比较差异无统计学意义 ($P > 0.05$)。见图5和6。

2.6 划痕损伤后各组大鼠脊髓星形胶质细胞中*Mfn2*蛋白表达水平 与Scratch 0 h组比较, Scratch 12、24和48 h组大鼠脊髓星形胶质细胞中*Mfn2*蛋白表达水平降低 ($P < 0.05$); 与Scratch 12 h组比较, Scratch 24和48 h组大鼠脊髓星形胶质细胞中*Mfn2*蛋白表达水平降低 ($P < 0.05$); 与Scratch 24 h组比较, Scratch 48 h组大鼠脊髓星形胶质细胞

中*Mfn2*蛋白表达水平降低 ($P < 0.05$)。见图7。

2.7 *Mfn2*与*miR-17-5p*之间的靶向调控关系

TargetScan 7.2 数据库预测 *miR-17-5p* 与 *Mfn2* mRNA的3'UTR区存在结合位点。双荧光素酶报告基因实验结果显示: 与mimics NC组比较, *miR-17-5p* mimics和*Mfn2*-WT共转染后*miR-17-5p* mimics组大鼠脊髓星形胶质细胞荧光素酶活性降低 ($P < 0.05$), *Mfn2*-MUT共转染后*miR-17-5p* mimics组大鼠脊髓星形胶质细胞荧光素酶活性无显著变化, 差异无统计学意义 ($P > 0.05$)。见图8。

2.8 抑制*miR-17-5p*后大鼠脊髓星形胶质细胞中*miR-17-5p*和*Mfn2* mRNA及蛋白表达水平

空白组、inhibitor-NC组和*miR-17-5p* inhibitor组大鼠脊髓星形胶质细胞中*miR-17-5p*表达水平分别为 1.00 ± 0.04 、 0.99 ± 0.03 和 0.25 ± 0.03 。与空白组比较, *miR-17-5p* inhibitor组大鼠脊髓星形胶质细胞中*miR-17-5p*表达水平降低 ($P < 0.05$), *Mfn2* mRNA和蛋白表达水平升高 ($P < 0.05$); 空白组与inhibitor-NC组大鼠脊髓星形胶质细胞中*miR-17-5p*和*Mfn2* mRNA及*Mfn2*蛋白表达水平比较差异无统

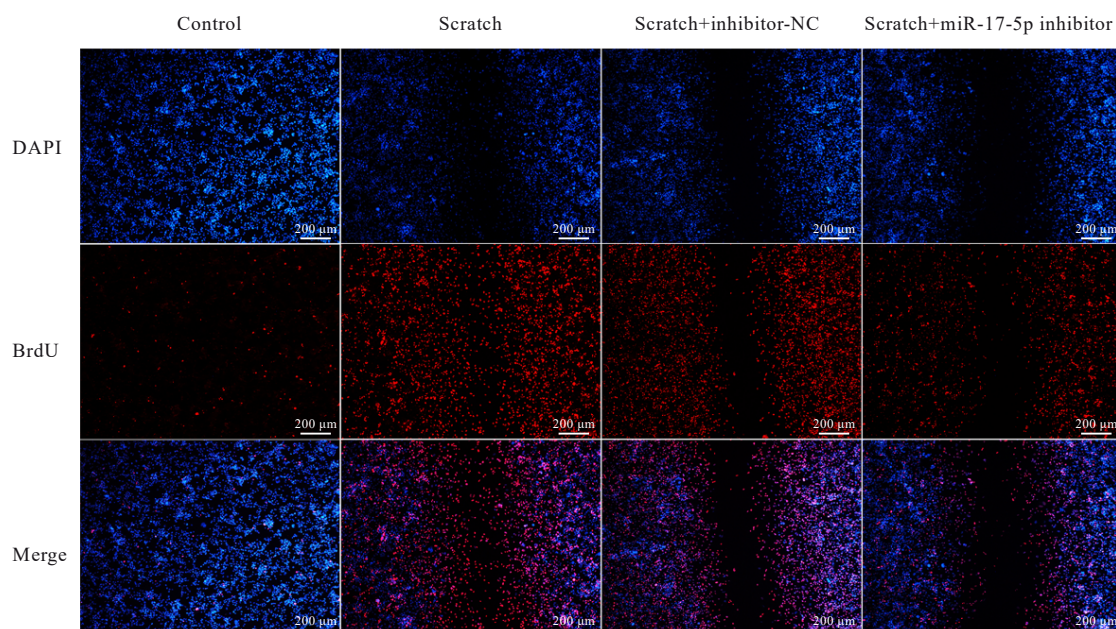
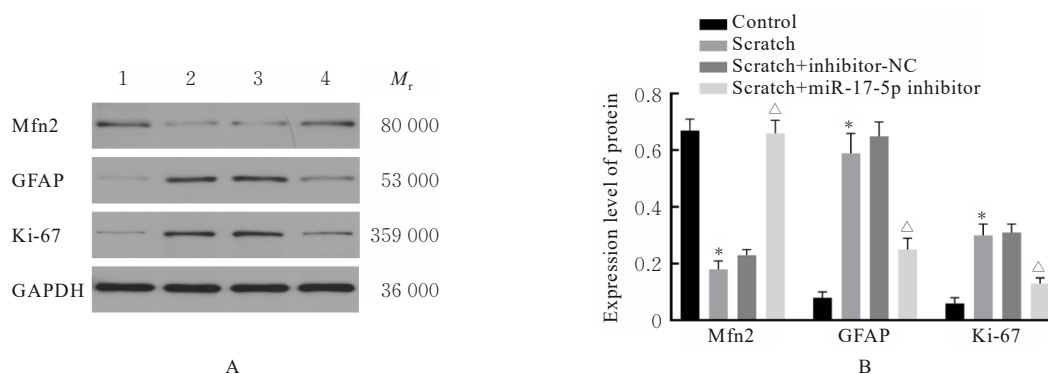


图5 各组大鼠脊髓星形胶质细胞中BrdU阳性表达情况

Fig. 5 Positive expressions of BrdU spinal cord astrocytes of rats in various groups



Lane 1: Control group; Lane 2: Scratch group; Lane 3: Scratch+inhibitor-NC group; Lane 4: Scratch+miR-17-5p inhibitor group.
* $P < 0.05$ compared with control group; $\Delta P < 0.05$ compared with scratch group.

图6 各组大鼠脊髓胶质细胞中Mfn2、GFAP和Ki-67蛋白表达电泳图(A)及直条图(B)

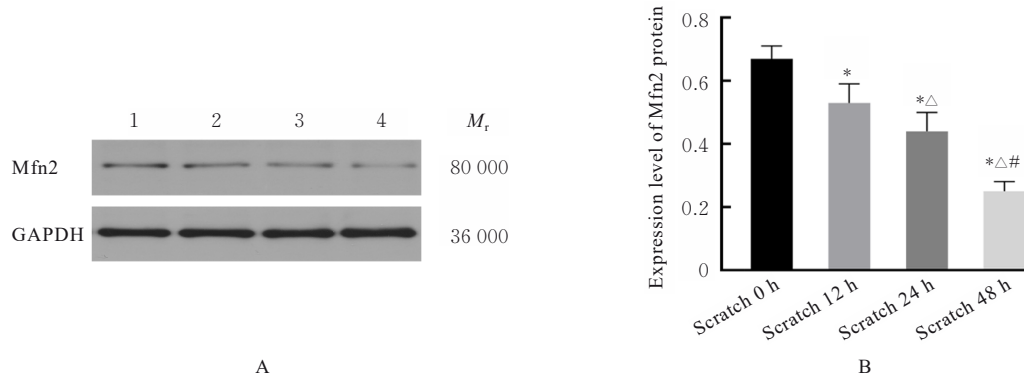
Fig. 6 Electrophoregram (A) and histogram (B) of expression of Mfn2, GFAP, and Ki-67 proteins in spinal cord astrocytes of rats in various groups

计学意义 ($P > 0.05$)。见图9。

2.9 沉默Mfn2并抑制miR-17-5p后大鼠脊髓星形胶质细胞中Mfn2蛋白表达水平 与对照组比较, Scratch组大鼠脊髓星形胶质细胞中Mfn2蛋白表达水平降低 ($P < 0.05$); 与Scratch组比较, Scratch+miR-17-5p inhibitor组大鼠脊髓星形胶质细胞中Mfn2蛋白表达水平升高 ($P < 0.05$); Scratch+inhibitor-NC组大鼠脊髓星形胶质细胞中Mfn2蛋白表达水平无显著变化, 差异无统计学意义 ($P > 0.05$); 与Scratch+miR-17-5p inhibitor组比

较, miR-17-5p inhibitor+si-Mfn2组大鼠脊髓星形胶质细胞中Mfn2蛋白表达水平降低 ($P < 0.05$), miR-17-5p inhibitor+si-NC组大鼠脊髓星形胶质细胞中Mfn2蛋白表达水平无明显变化, 差异无统计学意义 ($P > 0.05$)。见图10。

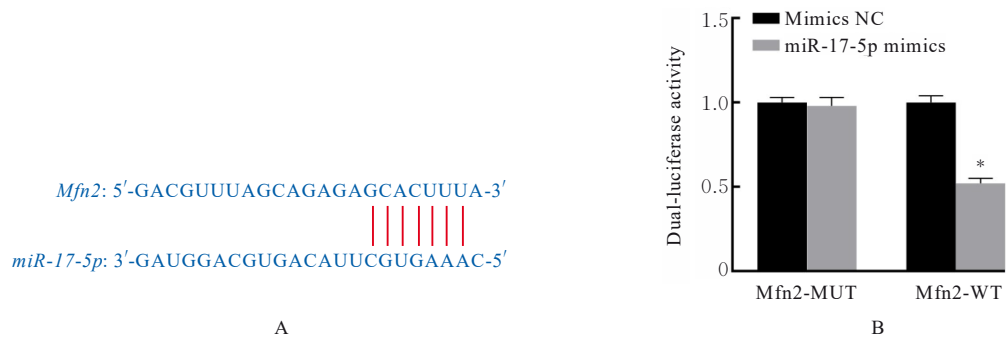
2.10 沉默Mfn2并抑制miR-17-5p后大鼠脊髓星形胶质细胞中BrdU阳性表达率以及GFAP和Ki-67免疫荧光共定位情况 对照组、Scratch组、Scratch+inhibitor-NC组、Scratch+miR-17-5p inhibitor组、miR-17-5p inhibitor+si-NC组和miR-17-5p



Lane 1: Scratch 0 h group; Lane 2: Scratch 12 h group; Lane 3: Scratch 24 h group; Lane 4: Scratch 48 h group; * $P < 0.05$ compared with scratch 0 h group; $\Delta P < 0.05$ compared with scratch 12 h group; # $P < 0.05$ compared with scratch 24 h group.

图 7 划痕损伤后各组大鼠脊髓星形胶质细胞中 *Mfn2* 蛋白表达电泳图(A)和直条图(B)

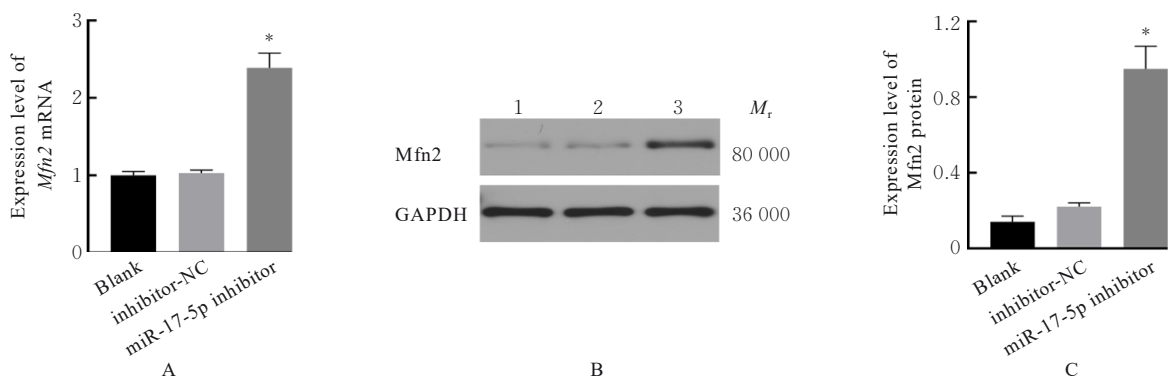
Fig. 7 Electrophoregram (A) and histogram (B) of expressions of *Mfn2* protein in spinal cord astrocytes of rats in various groups



A: Targeted binding sites between *Mfn2* and *miR-17-5p*; B: Dual luciferase activity. * $P < 0.05$ compared with mimics NC group.

图 8 *Mfn2* 与 *miR-17-5p* 之间的靶向调控关系

Fig. 8 Targeted regulatory relationship between *Mfn2* and *miR-17-5p*



Lane 1: Blank group; Lane 2: Inhibitor-NC group; Lane 3: miR-17-5p inhibitor group. * $P < 0.05$ compared with blank group.

图 9 各组大鼠脊髓星形胶质细胞中 *Mfn2* mRNA 表达水平(A)以及 *Mfn2* 蛋白表达电泳图(B)和直条图(C)

Fig. 9 Expression levels of *Mfn2* mRNA (A) and electrophoregram (B) and histogram (C) of *Mfn2* protein expression in spinal cord astrocytes of rats in various groups

inhibitor+si-Mfn2 组大鼠脊髓星形胶质细胞 BrdU 阳性表达率分别为 3.83%±0.50%、82.16%±7.73%、80.61%±6.74%、30.42%±2.86%、

31.56%±2.66% 和 64.58%±4.96%；GFAP 和 Ki-67 共定位细胞数量分别为 23.33±2.52、148.33±7.51、154.67±10.02、62.67±4.51、

59.33±4.04 和 117.67±6.03。与对照组比较, Scratch组大鼠脊髓星形胶质细胞中BrdU阳性表达率及GFAP与Ki-67共定位细胞数量增加($P<0.05$)。与Scratch组比较, Scratch+miR-17-5p inhibitor组大鼠脊髓星形胶质细胞中BrdU阳性表达率及GFAP与Ki-67共定位细胞数量减少($P<0.05$); Scratch+inhibitor-NC组大鼠脊髓星形胶质细胞中

上述指标无明显变化, 差异无统计学意义($P>0.05$)。与Scratch+miR-17-5p inhibitor组比较, miR-17-5p inhibitor+si-Mfn2组大鼠脊髓星形胶质细胞中BrdU阳性表达率及GFAP与Ki-67共定位细胞数量增加($P<0.05$); miR-17-5p inhibitor+si-NC组大鼠脊髓星形胶质细胞中无明显变化, 差异无统计学意义($P>0.05$)。见图11和12。

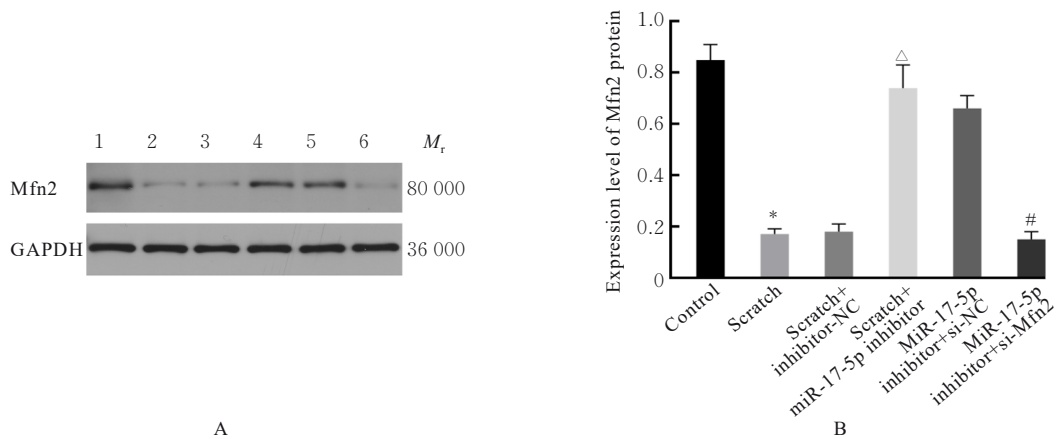


图10 各组大鼠脊髓星形胶质细胞中Mfn2蛋白表达电泳图(A)和直条图(B)
Lane 1: Control group; Lane 2: Scratch group; Lane 3: Scratch+inhibitor-NC group; Lane 4: Scratch+miR-17-5p inhibitor group; Lane 5: MiR-17-5p inhibitor+si-NC group; Lane 6: MiR-17-5p inhibitor+si-Mfn2 group. * $P<0.05$ compared with control group; [△] $P<0.05$ compared with scratch group; # $P<0.05$ compared with scratch+miR-17-5p inhibitor group.

图10 各组大鼠脊髓星形胶质细胞中Mfn2蛋白表达电泳图(A)和直条图(B)
Fig. 10 Electrophoregram (A) and histogram (B) of expressions of Mfn2 protein in spinal cord astrocytes of rats in various groups

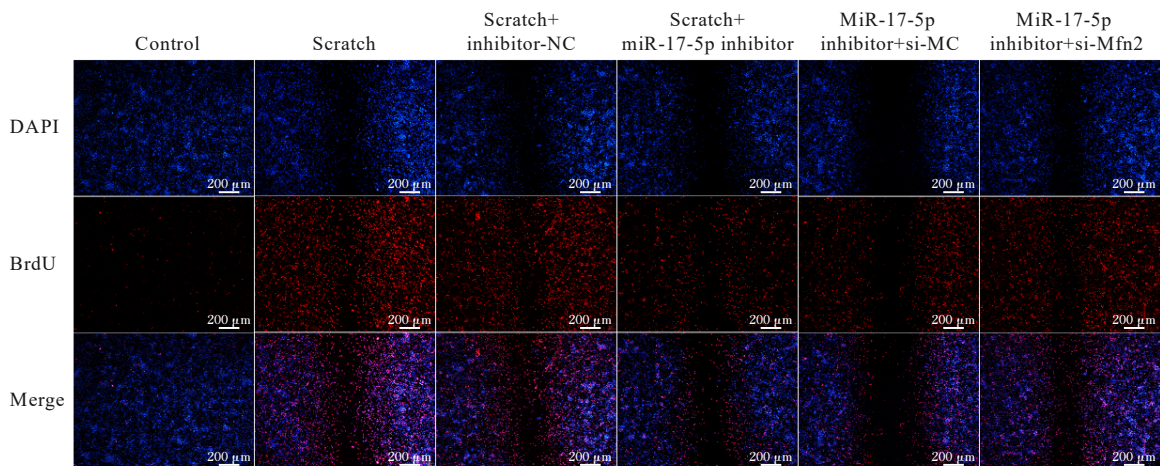


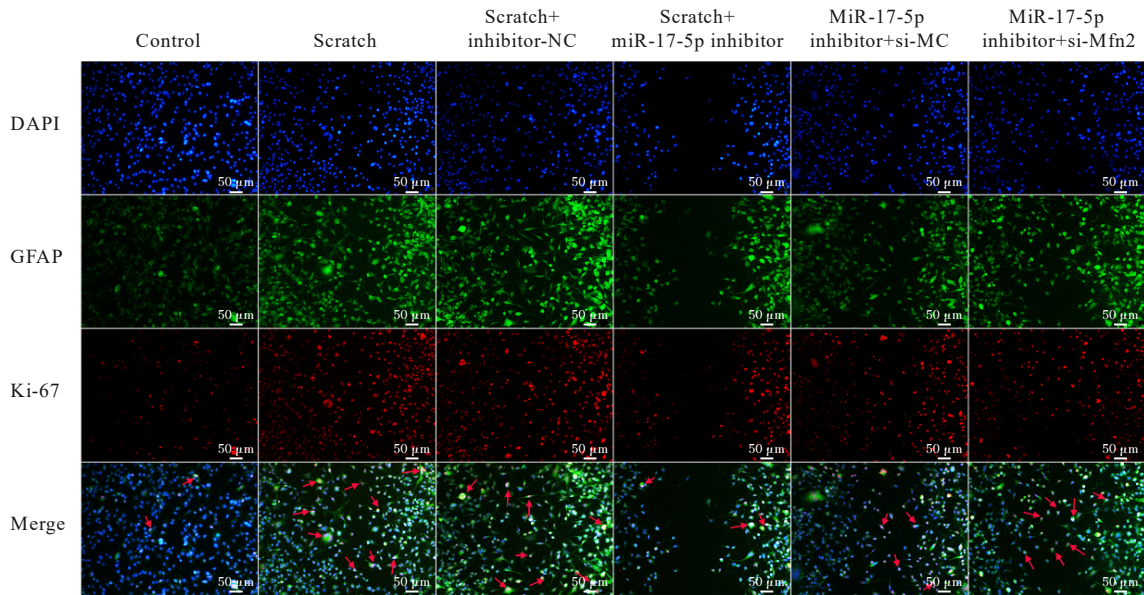
图11 各组大鼠脊髓星形胶质细胞中BrdU阳性表达情况

Fig. 11 BrdU positive expression in spinal cord astrocytes of rats in various groups

3 讨论

神经胶质瘢痕由细长的星形胶质细胞、成纤维细胞和分泌硫酸软骨素蛋白聚糖、胶原及致密细胞外基质的小胶质细胞组成, 作为物理化学屏障隔离

神经病变并在损伤中心隔离扩散性炎症、活性氧和兴奋性毒性以保护周围的健康组织, 但也不利于神经再生^[10-11]。脊髓损伤后, 各种细胞信号结合到损伤区域附近, 诱导神经胶质细胞群进入反应性增生



Arrows referred to GFAP and Ki-67 co-localized cells.

图 12 各组大鼠脊髓星形胶质细胞中 GFAP 与 Ki-67 免疫荧光共定位情况

Fig. 12 Immunofluorescence co-localization of GFAP and Ki-67 in spinal cord astrocytes of rats in various groups

状态, 在此期间, 星形胶质细胞被激活, 表达 GFAP 和波形蛋白等以稳定新形成的星形胶质细胞结构, 进而产生细胞外基质强化瘢痕结构^[12-13]。本研究结果显示: 随着划痕损伤时间的延长, 细胞中星形胶质细胞标志物 GFAP 以及细胞增殖蛋白 PCNA 和 Ki-67 表达水平逐渐升高, 表明划痕损伤后星形胶质细胞增殖能力增强, 抑制星形胶质细胞增殖可能是抑制脊髓损伤胶质瘢痕形成的有效途径。既往研究^[14-15]结果表明: *miR-21*、*miR-124* 和 *miR-26a* 等多个 miRNA 通过调控星形胶质细胞状态参与脊髓损伤过程, 其中过表达 *miR-21* 通过促进星形胶质细胞的分泌和增殖, 在脊髓损伤后的组织损伤修复中发挥作用; *miR-124* 通过吞噬途径抑制小胶质细胞和星形胶质细胞的激活促进脊髓损伤中的运动功能恢复; 而富含 *miR-26a* 的外囊泡通过抑制神经元中的磷酸酶和张力蛋白同源物 (phosphatase and tensin homologue, PTEN) 和糖原合成酶激酶 3 β (glycogen synthase kinase-3 β , GSK-3 β) 信号通路, 减少损伤部位的星形胶质细胞增殖, 促进轴突生长。本研究结果显示: 抑制 *miR-17-5p* 可下调划痕损伤后星形胶质细胞中的 GFAP 和 Ki-67 蛋白表达水平, 抑制细胞增殖。

Mfn2 是一种新发现的细胞增殖抑制基因, *Mfn2* 表达的下调使线粒体融合和分裂失衡, 通过诱导线粒体 DNA 的释放, 介导环鸟苷酸-腺苷酸合

成酶-干扰素基因刺激蛋白 (cyclic GMP-AMP synthase-stimulator of interferon genes, cGas-Sting) 信号通路激活, 进而加重脊髓损伤后的炎症反应^[16-17]。SHI 等^[18] 研究表明: 在体外氧-葡萄糖剥夺/再氧合诱导的反应性星形胶质细胞中, *Mfn2* 基因和蛋白表达水平均显著下调, 过表达 *Mfn2* 可抑制氧-葡萄糖剥夺/再氧合诱导的星形胶质细胞增殖。而本研究结果显示: 随着划痕损伤时间的延长, 星形胶质细胞中 *Mfn2* mRNA 和蛋白表达水平逐渐降低, 与 LIU 等^[19] 研究结果一致。既往研究^[20-21] 结果表明: *miR-17-5p*/*Mfn2* 信号通路通过平衡氧化还原、抑制胶原纤维沉积和炎症等途径对缺氧-再灌注损伤心肌细胞和非酒精性脂肪肝发挥保护作用, 以上研究提示 *miR-17-5p* 可能通过调控 *Mfn2* 表达来调控星形胶质细胞增殖状态。本研究通过生物信息学网站预测 *miR-17-5p* 与 *Mfn2* 的靶向结合位点, 并验证了 *Mfn2* 是 *miR-17-5p* 的下游靶基因; 同时, *miR-17-5p* 下调可促进 *Mfn2* 表达, 而沉默 *Mfn2* 则会逆转下调 *miR-17-5p* 对划痕损伤诱导星形胶质细胞增殖的抑制作用, 表明下调 *miR-17-5p* 是通过靶向调控 *Mfn2* 表达来抑制机械损伤诱导的星形胶质细胞增殖。

综上所述, 星形胶质细胞增殖是脊髓损伤后胶质瘢痕形成的主要原因, 下调 *miR-17-5p* 可通过靶向调控 *Mfn2* 表达抑制机械损伤诱导的星形胶质

胞增殖, 为以 *miR-17-5p* 为靶点的脊髓损伤治疗药物开发提供了依据, 本课题组将继续通过动物实验从体内水平验证此结论。

利益冲突声明:

所有作者声明不存在利益冲突。

作者贡献声明:

赵焱参与实验操作、数据处理和论文撰写, 吴华伟参与实验设计、数据分析、写作指导和论文审阅。

[参考文献]

- [1] IZZY S. Traumatic spinal cord injury [J]. *Continuum*, 2024, 30(1):53-72.
- [2] ANJUM A, YAZID M D, FAUZI DAUD M, et al. Spinal cord injury: pathophysiology, multimolecular interactions, and underlying recovery mechanisms [J]. *Int J Mol Sci*, 2020, 21(20):7533.
- [3] MAO H, CHEN W, CHEN L X, et al. Potential role of mitochondria-associated endoplasmic reticulum membrane proteins in diseases [J]. *Biochem Pharmacol*, 2022, 199:115011.
- [4] CAO Y, LV G, WANG Y S, et al. Mitochondrial fusion and fission after spinal cord injury in rats [J]. *Brain Res*, 2013, 1522:59-66.
- [5] SHI Y L, LUO P, YI C L, et al. Effects of Mitofusin2 on astrocytes proliferation *in vitro* induced by scratch injury [J]. *Neurosci Lett*, 2020, 729:134969.
- [6] HONG P W, JIANG M, LI H D. Functional requirement of dicer1 and miR-17-5p in reactive astrocyte proliferation after spinal cord injury in the mouse [J]. *Glia*, 2014, 62(12):2044-2060.
- [7] ZHANG L, WANG Z J, LI B, et al. The inhibition of miR-17-5p promotes cortical neuron neurite growth *via* STAT3/GAP-43 pathway [J]. *Mol Biol Rep*, 2020, 47(3):1795-1802.
- [8] MISHRA P S, RAJU T R. A simple and efficient method for concomitant isolation and culture of enriched astroglial and microglial cells from the rat spinal cord [J]. *Bio Protoc*, 2020, 10(2):e3501.
- [9] CAI J J, KONG J D, MA S, et al. Upregulation of TRPC6 inhibits astrocyte activation and proliferation after spinal cord injury in rats by suppressing AQP4 expression [J]. *Brain Res Bull*, 2022, 190:12-21.
- [10] ORR M B, GENSEL J C. Spinal cord injury scarring and inflammation: therapies targeting glial and inflammatory responses [J]. *Neurotherapeutics*, 2018, 15(3):541-553.
- [11] MARANGON D, CASTRO E SILVA J H, CERRATO V, et al. Oligodendrocyte progenitors in glial scar: a bet on remyelination [J]. *Cells*, 2024, 13(12):1024.
- [12] 刘建春, 张红珍, 王青, 等. 黄芪甲苷对EAE小鼠轴突修复和再生的促进作用机制 [J]. *解放军医学杂志*, 2024, 49(8):914-921.
- [13] GONG L L, GU Y, HAN X X, et al. Spatiotemporal dynamics of the molecular expression pattern and intercellular interactions in the glial scar response to spinal cord injury [J]. *Neurosci Bull*, 2023, 39(2):213-244.
- [14] YANG R C, YANG B, LIU W, et al. Emerging role of non-coding RNAs in neuroinflammation mediated by microglia and astrocytes [J]. *J Neuroinflammation*, 2023, 20(1):173.
- [15] GAO X, LI S Y, YANG Y J, et al. A novel magnetic responsive miR-26a@SPIONs-OECs for spinal cord injury: triggering neural regeneration program and orienting axon guidance in inhibitory astrocytic environment [J]. *Adv Sci (Weinh)*, 2023, 10(32):e2304487.
- [16] WEI F L, WANG T F, WANG C L, et al. Cytoplasmic escape of mitochondrial DNA mediated by Mfn2 downregulation promotes microglial activation *via* cGas-sting axis in spinal cord injury [J]. *Adv Sci (Weinh)*, 2024, 11(4):e2305442.
- [17] HSU C C, WU K L H, PENG J M, et al. Low-energy extracorporeal shockwave therapy improves locomotor functions, tissue regeneration, and modulating the inflammation induced FGF1 and FGF2 signaling to protect damaged tissue in spinal cord injury of rat model: an experimental animal study [J]. *Int J Surg*, 2024, 110(12):7563-7572.
- [18] SHI Y L, YI C L, LI X, et al. Overexpression of Mitofusin2 decreased the reactive astrocytes proliferation *in vitro* induced by oxygen-glucose deprivation/reoxygenation [J]. *Neurosci Lett*, 2017, 639:68-73.
- [19] LIU T, XUE C C, SHI Y L, et al. Overexpression of mitofusin 2 inhibits reactive astroglial proliferation *in vitro* [J]. *Neurosci Lett*, 2014, 579:24-29.
- [20] LI Q, BU Y L, SHAO H F, et al. Protective effect of bone marrow mesenchymal stem cell-derived exosomes on cardiomyoblast hypoxia-reperfusion injury through the HAND2-AS1/miR-17-5p/Mfn2 axis [J]. *BMC Cardiovasc Disord*, 2023, 23(1):114.
- [21] 李聪, 刘小慧, 熊海容, 等. 竹节参皂苷IVa调节miR-17-5p/MFN2信号通路改善非酒精性脂肪性肝炎 [J]. *中国中药杂志*, 2020, 45(19):4725-4731.